Optica Applicata, Vol. XXIX, No. 1–2, 1999

Sensing applications of fiber-optic Sagnac interferometer

LESZEK R. JAROSZEWICZ, ALEKSANDER KIEŻUN, RYSZARD ŚWIŁŁO

Institute of Applied Physics, Military University of Technology, ul. Kaliskiego 2, 00–908 Warszawa, Poland.

The various possible applications of the fiber-optic Sagnac interferometer as a sensor of physical fields are presented. The use of the Sagnac interferometer as an optical gyroscope for an investigation of slow-speed rotational platforms and a construction of distributed security system are described. The possibilities of applying a modified system for measurements of nanometer vibrations and parameters of the in-line fiber-optic polarizer, phase and polarisation modulator are also presented. Finally, the usability of the Sagnac interferometer as a fiber-optic ellipsometer is described.

1. Introduction

The fiber-optic Sagnac interferometer (FOSI) has been in use for twenty years now. The first, and probably the most spectacular, application of this device is optical gyroscope [1]. However, other possibilities of FOSI application have been developed in the last ten years. The main of them are: distributed security systems, current and magnetic sensors, and systems for monitoring large objects [2]. In every case, advantage is taken of the fundamental property of the FOSI, *i.e.*, good stability of system operation. It is of vital importance that one piece of a fiber can be used as a medium for propagation of two beams (in opposite directions). This approach solves the prolems of coherence because the interacting beams always have the same optical length. Therefore, a slow coherence source can be used. The fact of optical ways being identical for two beams renders it also possible to minimise any effect the environment might have on operation of the system.

In this paper, a review of our works concerning the understanding of the FOSI is presented. Other practical applications of the FOSI based on the first Polish fiber-optic gyroscope [3] are presented.

2. Polarisation behaviour of the FOSI

Optical fibers and fiber-optic elements, in general, exhibit variable birefringence. In the case of application to construction of an interferometric system, it causes the polarisation effect on interference phenomena. On the contrary, optical paths of classic interferometers are usually isotropic or exhibit constant birefringence. This

is the main difference between bulk- and fiber-optic interferometers. For those reasons, it is coherence for the first kind of interferometer and polarisation for the second one that have the main influence on the system operation [4], [5].

The best way to take into consideration the changes of polarisation in fiber-optic system is the Jones' calculus. In this formalism, the interferometer transfer function for all fiber-optic interferometer configurations (Fig. 1) may be described as [6]

$$I = 0.5[1 \pm V\cos(\varphi + \varphi_0)], \quad V = \mathrm{abs}(m), \quad \varphi_0 = \arg(m) \tag{1a}$$

where

$$m = \mathbf{E}^{+}\mathbf{M}_r^{+}\mathbf{M}_s\mathbf{E} \tag{1b}$$

is dependent on polarisation behaviour of input beam (described by the Jones' vector **E**) and reference and signal arms of interferometer (described by the Jone's matrices $\mathbf{M}_r$ and $\mathbf{M}_s$), respectively. In the above notation, V describes the scale factor while the phase coefficient is a sum of phase disturbance φ generated in a given configuration and additional shift φ_0 (bias). The first parameter is directly proportional to the system sensitivity, the second depends on configuration, and its slow change in time is usually classified as a drift. Moreover, the upper sign "+" describes the Hermite-conjugate system operation.

A classification of fiber-optic systems, introduced in Fig. 1, as the in-directional interferometer (IDI) and the counter-directional interferometer (CDI) is connected

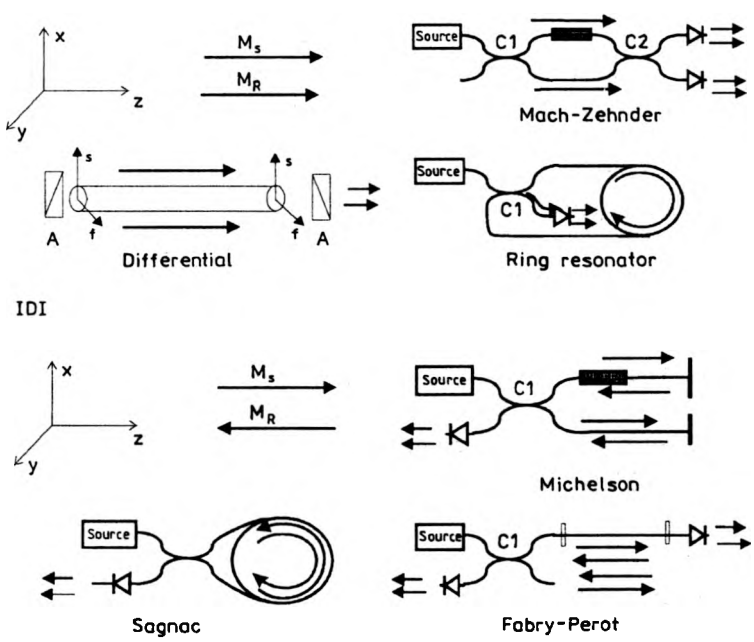

Fig. 1. Classification of fiber-optic interferometers: IDI – in-directional interferometry system, CDI – counter-directional interferometry system, C1, C2 – couplers, ×N – multi-path ways, A – polarizer.

with their mathematical description [4]. The essential difference in the description of the second group is the necessity of introducing matrices that describe a passage through a given element or group of elements in the direction opposite to the assumed reference system. If the Jones' matrix describing a given element is a unimodular matrix **M**, then passage in the opposite direction is described by transposed matrix $\mathbf{M}^T$. To enhance polarisation properties we can describe optical fiber by means of the Kapron's rule of equivalence. According to this rule, any unknown fiber-optic system can always be treated as a set of three discrete elements: rotator with axes χ – rotator $\mathbf{R}(\chi)$, linear phase retarder of retardation δ – rotator $\mathbf{G}(\delta)$, and circular retarder introducing rotation of angle ζ. Circular rotator introduces circular polarisation states and is described in the Cartesian system by rotator matrix $\mathbf{R}(\zeta)$. Hence, a description of any fiber-optic path gives the Jones' matrix of the following general form:

$$\mathbf{M} = \begin{bmatrix} m_{11} & m_{12} \\ m_{21} & m_{22} \end{bmatrix} = \mathbf{R}(\zeta)\mathbf{G}(\delta)\mathbf{R}(\chi). \tag{2}$$

The extended investigation of different interferometric configurations with respect to their polarisation behaviour has been done in [4], [5]. Here we summarise only the main conclusions concerning the FOSI. This configuration as a double-beam system includes all other configurations shown in Fig. 1. The system is the CDI as for the Michelson system, but it is also balanced (as in the differential interferometer, propagation takes place in one optical fiber only). Moreover, the signal path is described by the Kapron's model, in the same way as for the Mach–Zehnder system. The existence of a single coupler in the system causes that distribution of output power is analogous to that for the Michelson configuration.

According to the matrix description of the FOSI operation, we can obtain the parameter m for a system with a transducer placed close to a coupler as

$$m = \mathbf{E}^+ \mathbf{R}(\zeta)\,\mathbf{G}(-\delta)\,\mathbf{R}(\chi+\zeta)\,\mathbf{G}(\delta)\,\mathbf{R}(\chi)\mathbf{E}, \tag{3}$$

which shows that the system operation depends on input state of polarisation (SOP) also. This input SOP described in the Jones formalism as the vector

$$\mathbf{E} = \begin{bmatrix} E_x \\ E_y \end{bmatrix} = \begin{bmatrix} \cos\Phi \\ \sin\Phi e^{j\Delta} \end{bmatrix} \tag{4}$$

depends on the SOP parameters such as the diagonal angle Φ and retardation of the electric field orthogonal components Δ.

It results from the above dependence that if only one factor exists which causes rotation of polarisation plane ($\delta = 0$, $\mathbf{M}_s = \mathbf{R}(\alpha)$), the following simple analytical dependences can be obtained:

$$V = \sqrt{\cos^2(2\alpha) + \sin^2(2\alpha)\sin^2(2\Phi)\sin^2\Delta}, \quad \varphi_0 = \tan^{-1}[-\tan(2\alpha)\sin(2\Phi)\sin\Delta]. \tag{5a}$$

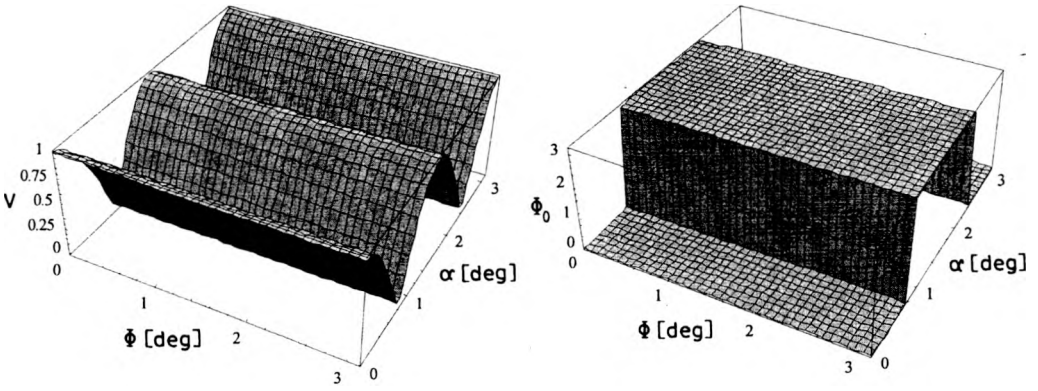

Fig. 2. Sensitivity V and bias φ_0 in the case of the FOSI with fiber rotation α, excited by linear polarised beam with variable angle Φ [5].

This result shows that for any SOP of input beam, changes of the sensitivity and the drift take place. Applying the input polarisation filter (fiber-optic polarizer placed in front of the input coupler), which excites the system by a linearly polarised beam, causes, according to Fig. 2, that rotation brings about only a change of the system sensitivity.

On the other hand, if only linear birefringence is observed ($\chi = \zeta = 0$, $\mathbf{M}_s = \mathbf{G}(\delta)$), one can obtain the following expression:

$$V = 1, \quad \varphi_0 = 0, \tag{5b}$$

which means that the FOSI is insensitive to the pure linear birefringence.

The above special properties of this configuration stem from the fact that only one fiber is used as a path for both interacting beams. Due to their counter-running propagation, the effect of linear birefringence is neutralised. This results from that, independent of the SOP of the excited beam at an arbitrarily chosen point along a loop, both beams exhibit the same SOP. According to the phenomenological description [4] such a situation causes the sharpest interference contrast.

On the other hand, the existence of a factor making polarisation plane rotate in a fiber affects both beams in the same way. Therefore, for the rotation by $\pi/4$ both interacting beams are perpendicular at the output and the sensitivity falls to zero (see left part of Fig. 2). If a rotation angle is equal to $\pi/2$, which is the case of signal vanishing in the Mach–Zehnder system [5], the output beams in the loop interferometer are rotated by an angle π. In other words, output beams are parallel and therefore the sensitivity is the highest. A phase is also shifted by π, but this fact causes no change in the transfer function of the system. Introduction of a fiber optic polarizer at the input of this configuration causes filtration of polarisation – only one mode is excited ($\Phi = n\pi/2$) and a light way is common to the input and output. According to (5b), the vanishing of bias takes place then. In this case, variable polarisation properties of a system do not cause a drift. Such a configuration,

usually described as the minimum configuration of the system [7], forms a basis for constructing a fiber-optic gyroscope.

3. Application of the FOSI to rotation sensing

The application of the FOSI for detection of rotation speed, especially as a fiber-optic gyroscope (FOG), is probably the most attractive proposition as regards fiber-optic sensors. The operation of this system is based on the so-called Sagnac effect. This effect, based on the loop optical interferometer, consists in the generation of a phase or frequency shift proportional to the rotation velocity. In the case of the FOSI, the phase shift generated in the system is described as

$$\varphi = \frac{4\pi RL}{\lambda c} \varkappa \Omega \tag{6}$$

where R is the radius of the sensor loop, L is the length of optical fibers in the loop, λ is the wavelength of light, c is the light speed in vacuum, $\varkappa$ is the conversion coefficient, which depends on parameters of the electronic treatment of the signal, and Ω is the rotation speed component in the direction perpendicular to the loop plane.

The above application of fiber-optic snsor is so popular that fiber-optic interferometer in loop configuration is usually wrongly named the Sagnac interferometer.

3.1. Research and development of the FOG

The main investigations of the FOG were conducted in our laboratory more than ten years ago. In general, all works concerned construction of two axis devices for application to military automobile. The optical unit of this device was made in conformity with minimum configuration shown in Fig. 3.

The basic system, named SGS-13, was made by winding 380 m long PANDA fiber in the form of loop with a radius of 0.1 m. As the source, the semiconductor diode CQF-56 made by Philips has been used. This multimode CW laser ensures about

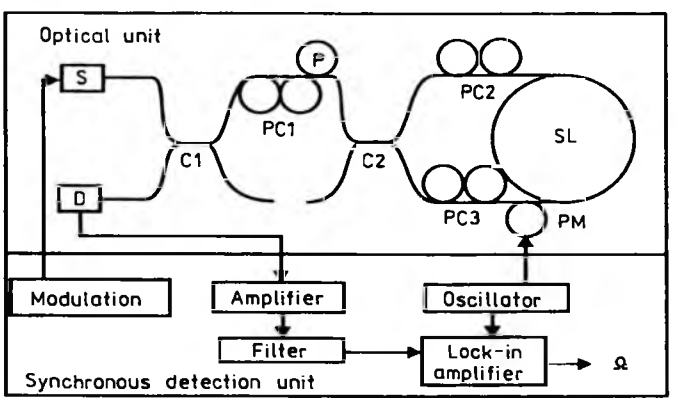

Fig. 3. Simplified FOG scheme. In optical unit: S – source, C1, C2 – couplers, P – polarizer, PC – polarisation controller, SL – sensing loop, PM – phase detector

1 mW output power on a pig-tailed single-mode fiber for 1300 nm wavelength. The fiber of the same kind wound on the piezoceramic cylinder of 0.08 m in diameter was applied as a phase modulator PM used for synchronic detection. The required quadrate point of system work was obtained for 144 kHz and 0.85 V signal steering the PM. The experimental investigation of this system has shown that its sensitivity is in range of 0.25 deg/h (see Fig. 4), and its drift is about 5 deg/h.

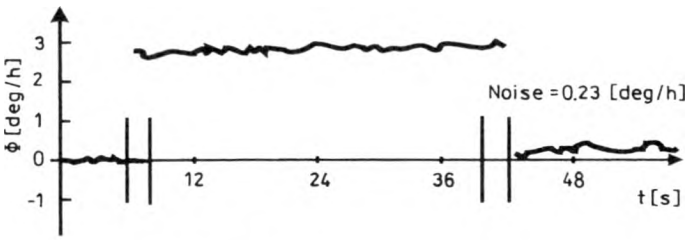

Fig. 4. Sensitivity of SGS-13 [3].

The fundamental system investigation, based on the Jones' matrix calculus, showed the main influence on drift to be due to diversification of fiber-optic elements used [3]. We employed the HiBi fiber in sensor loop SL, phase modulator PM and polarizer P. Other optical elements are made on the standard single-mode optical fiber base for the economical reason. This solution caused a mismatch of birefringence axes in element connections. The simulation showed that especially sensitive were connections of the coupler with polarizer and the coupler with the sensor loop end. Therefore, we used three polarisation controllers PC placed in front of the polarizer and at two ends of fiber loop. Unfortunately, such a solution can be used in laboratory system only.

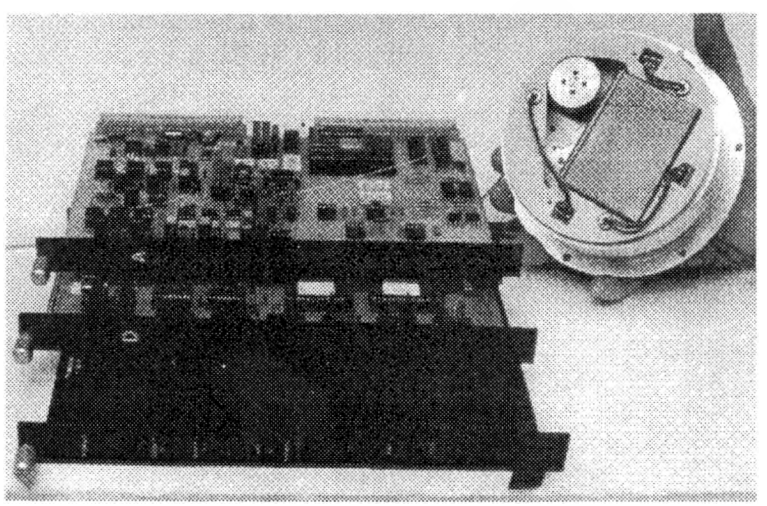

Fig. 5. View of one channel of DGS-13 together with specially developed electronic cards containing all necessary digital, analogue and thermo-stability circuits [9].

The constructed prototype of two-channel FOG named DGS-13 is shown in Fig. 5. In this device, a standard single-mode optical fiber for wavelength 1.3 μm has been used. We employed all fiber-optic elements made in our laboratory of Physics Application Department. The application of polarisation controller of a new kind [8] together with thermo-stability system gives the more useful device. Its main parameters include: the sensitivity of 1 deg/h, drift of 5 deg/h, maximum detected rotation speed 100 deg/s, and linearity in measurement band about 0.5%.

In spite of receiving the bronze medal at the International Exhibition IENA'94 in Nurnberg, this device has no commercial application yet. Nevertheless, all knowledge gained during its construction has been used for developing a wide range of other FOSI applications shown below.

3.2. Investigation of slow-speed platforms

Research into the quality TOTEM (used by I-22 aircraft), LTN-101 (An-28 aircraft) or LCR-92 (made by Air Force Technical Institute – AFTI) systems needs a suitable class of slow-speed platforms, used as standard source of angular velocity. However, from observation of the operation of the stands existing in Poland, it follows that the angular velocity generated by them has disturbances increasing with a decrease of average velocity generated by the stand. Until now the only method of measurements of those oscillations has been an observation of a shift of light spot used as an indicator of the uniformity of rotary movement. Another solution to this problem is an application of the optoelectronic sensor to measure real oscillations of those stands. Thus, a suitable single-channel FOG has been used for measurements.

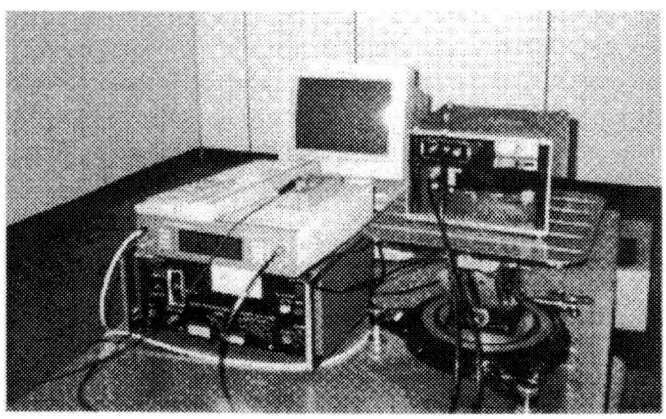

Fig. 6. GS-13P on stand for Eearth rotation measurement.

To measure the instantaneous velocity generated by slow-speed stands the SGS-13 system has been adopted [10]. This system described as GS-13P has modified optical head, signal processing system based on EG&G lock-in 7260 type, and IBM PC with special software (see Fig. 6). The main parameters of the adopted system are: sensitivity of 0.2 deg/h, wide measuring range up to 100 deg/s,

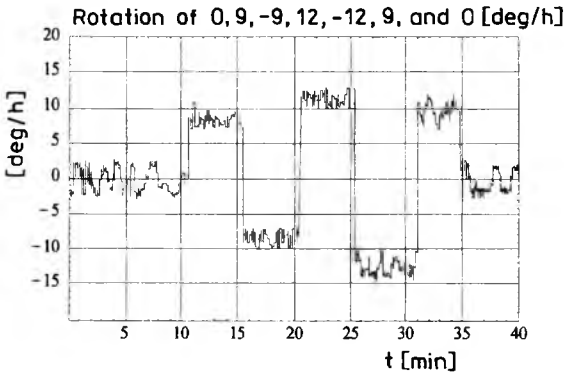

Fig. 7. Earth revolution measured by GS-13P.

transmission bandwidth up to 100 Hz, and drift of 5 deg/h. Due to this drift, such a system cannot be used for long-term studies. However, for short-term studies of the order of one minute, the drift is less than 0.08 deg/h. In this way, the system can be used for registration of real parameters of the motion generated by a given slow-speed stand with 0.2 deg/h resolution. Examples of the measurement of the Earth revolution components (horizontal North of 9 deg/h, and vertical one of 12 deg/h) for Warsaw are presented in Fig. 7.

Special software based on integral method renders it possible to calculate scale factor and other technical parameters of GS-13P system (according to PrPN-V-82002 standard). This method determines gyro and electronic constants on the basis of angular motion analysis which is done at different rotation speeds [10]. Moreover, this software enables the Earth revolution component to be removed, because it is constant for each measurement (+12 deg/h) and the sense of the measuring table revolution remains the same as for this component.

The measurements of angular velocity generated by such stands as: UPG-48, UPG-56 (used by Polish Air Force), SPB-1, SZK-1 (constructed by AFTI) and

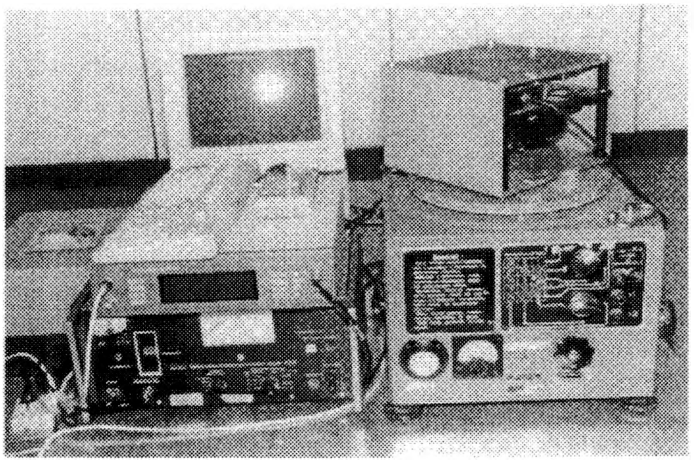

Fig. 8a

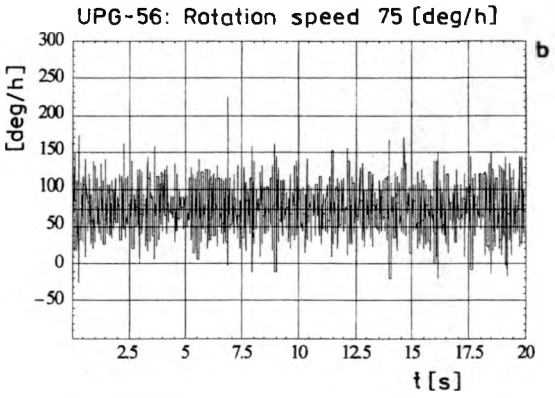

Fig. 8b

Fig. 8. UPG-56 (**a**) during measurements and the results (**b**) obtained for its lowest rotation speed generated.

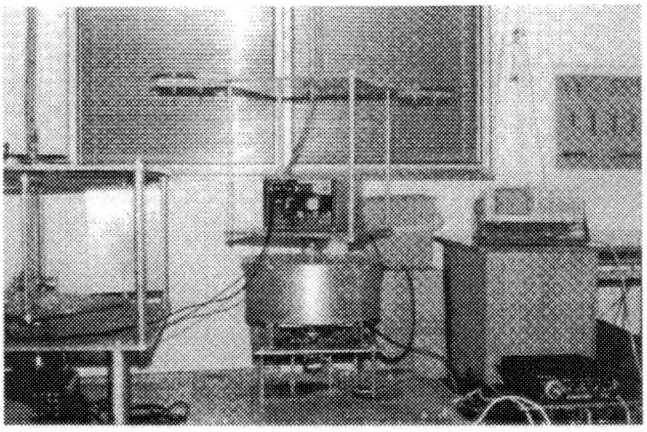

Fig. 9a

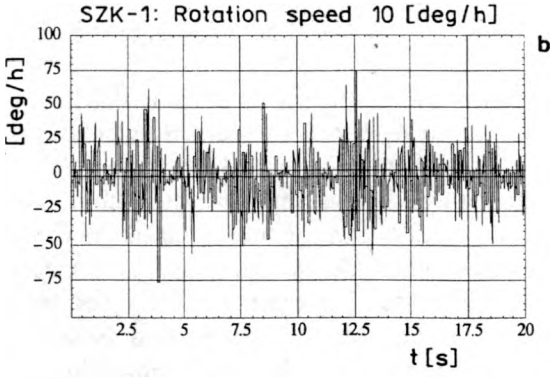

Fig. 9b

Fig. 9. SZK-1 (**a**) during measurements and the results (**b**) obtained for its lowest rotation speed generated.

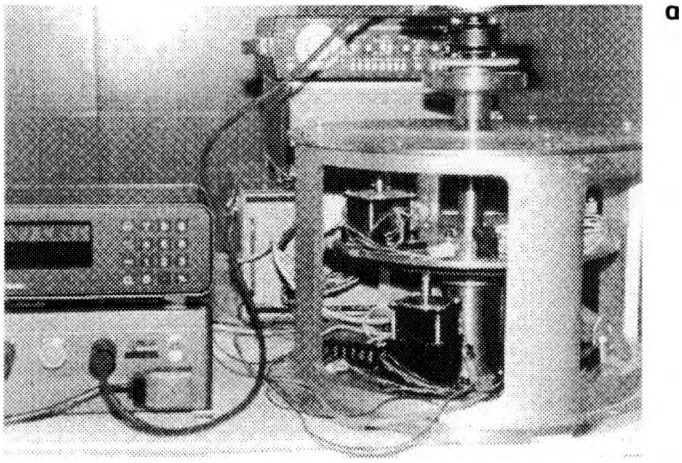

a

Fig. 10a

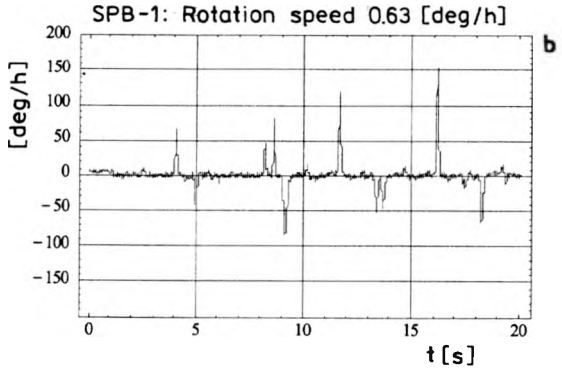

b

Fig. 10b

Fig. 10. SPB-1 (**a**) during measurements and the results (**b**) obtained for its lowest rotation speed generated

M13-04DC (made by COBRABiD Optica) have been made using the above system. The representative results are shown in Figs. 8 – 10 for UPG-56, SZK-1, and SPB-1, respectively [11].

During all measurements mentioned above, the platforms have rotated with the same mean angular velocity as the one predicted from the theoretical calculations. Unfortunately, the stands exhibit large disturbances, much higher than their expected level. An analysis of those disturbances shows their periodic character. Their sources are workmanship deviations, which can be observed as periodic nonuniformities of the motion generated. To define the disturbance sources, a special method has been worked out [10], [12] for extracting main disturbances from measured signals as well as modelling of platforms work. This method based on numerical simulation of mechanical construction of stands, offers possibility of analysing their angular velocity oscillations. Examples of such investigation are shown in Fig. 11, where simulation and experimental results are compared. As one

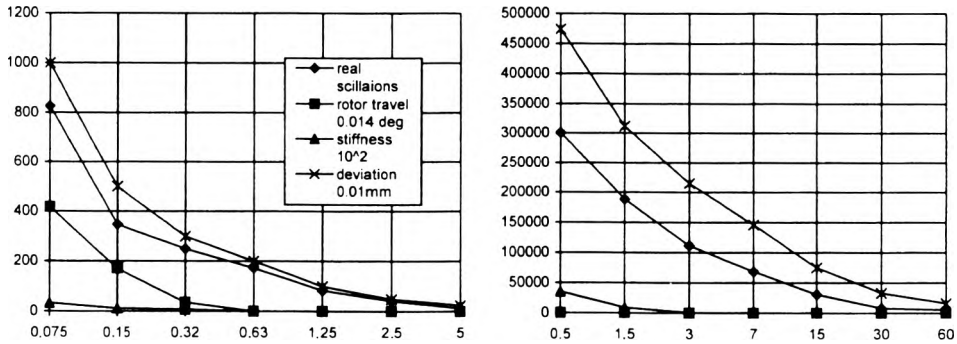

Fig. 11. Level of the measuring table oscillations [%] as a function of the disturbances and mean velocity for single-stage (Fig. **a**, [deg/s]) and double-stage (Fig. **b** [deg/h]) SPB-1 stand [11].

can see, the effect of simulation of the workmanship deviations of an order of 0.01 mm is in good agreement with the experimental results obtained from measurements of the rotor and the measuring table eccentricity.

The results obtained have shown the usefulness of the fiber-optic gyroscope to study properties of the slow-speed platforms. This method, the only one in Poland, enables registration of the real angular velocity, especially for the low velocity values.

3.3. Interferometric measurement of fiber-optic polarizer extinction ratio

The investigation of the FOG has been connected with developing in our laboratory the basis for new fiber-optic elements. An in-line biconical taper fiber polarizer was one of them. The measurement of its fundamental parameter – extinction ratio has been difficult due to its high value. Therefore, a new interferometric method has been worked out [13]. The method uses a dependence of FOG drift on polarizer quality. The FOG investigation has shown that main source of the drift is connected with disturbances of phase relation between polarisation modes [7]. These disturbances may be eliminated by the polarizer with extremely high extinction ratio. Certainly, the imperfection of polarizer is not the only source of the drift. Slow-change disturbances of external conditions, especially temperature, the Kerr effect and an external magnetic field are the other main sources of the drift. However, those effects may be minimised in laboratory condition to a level of 0.01 deg/h by application of thermo-stability, an input X-type coupler with 50% power division and a screening of the interferometer.

The effect of the polarizer with the extinction ε on FOG drift can be examined by using the Jones' matrix calculus. In this formalism the polarizer is described as

$$\mathbf{P} = \begin{bmatrix} 1 & 0 \\ 0 & \varepsilon \end{bmatrix}. \tag{7}$$

Then from (1) on the basis of (2), (4) and (7) the relation between bias value and

polarizer extinction ratio may be obtained as [14]

$$\varphi_0 = 2\varepsilon \frac{|E_y|}{|E_x|} \frac{|m_{12}|}{|m_{11}|} \tag{8}$$

where $\varepsilon|E_y|$ stands for an amplitude of y-mode extinction by polarizer, while $|m_{12}|$ means the amplitude of the wave propagating across the loop along the polarizer x-axis if input wave has been parallel to the y-axis. On the other hand, $|m_{11}|$ means the amplitude of the wave propagating across the loop in x-mode (input and output states are the same).

It is known that the phase shift φ generated by fiber-optic gyroscope is dependent on angular velocity Ω by relation (6). Then, if rotation speed is absent ($\Omega = 0$), the velocity measured by the system describes according to (1) the value of phase shift φ_0. The latter parameter is, on the basis of (8), a measure of the extinction level of polarizer applied.

Hence, the application of the system for a measurement of the extinction level requires an estimation of parameters existing on the right-hand side of identity (8). Because in the FOG system, semiconductor lasers coupled with single-mode fiber are used as light sources, one may find from catalogue data that $2|E_y|/|E_x| \sim 10^{-1}$. The main problem is an estimation of the value of $|m_{12}|/|m_{11}|$ ratio, which may be solved by introducing the polarisation controller (see Fig. 3). In other words, interferometer matrix is modified in such a way that $|m_{12}| = |m_{11}|$. In this case, identity (8) directly describes extinction level ε as the magnitude of bias. Therefore, the limit extinction of the polarizer may be obtained by comparison between (8) and (6). It should be underlined that the term "limit extinction" means that the extinction of polarizer under study is not lower than that obtained by the above described method.

In the experiment, four fiber-optic polarizers have been used. Three of them have been made in our laboratory while the last one has been obtained from YORK Co.

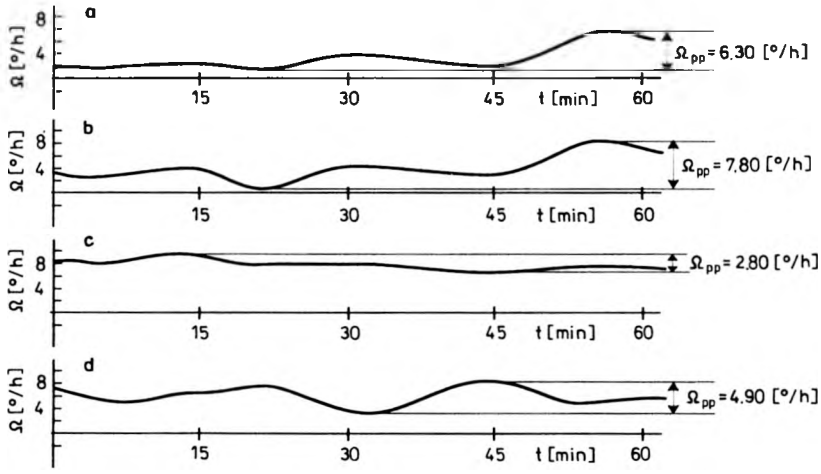

Fig. 12. Measurement of the drift velocity Ω and the peak-to-peak value for four different polarizers: **a**, **b**, **d** — made in the IAP MUT, **c** — made by YORK (GB), [13].

As measurement set-up, the fiber-optic gyroscope SGS-13 type has been applied. By placing the system on a special measurement set-up the effect of Earth revolution could be eliminated, which made it possible to register the drift in one-hour time intervals. The drift of fiber-optic gyroscope registered in this way for polarizers under study (see Fig. 12) equalled 6.30 deg/h, 7.80 deg/h, 4.90 deg/h and 2.80 deg/h for Polish and English polarizers, respectively. It is worth mentioning that the value Ω measured by this method should be defined as peak-to-peak value, *i.e.*, between maximum and minimum values, as shown in Fig. 12. The obtained values of drift after recalculation on the basis of (6) and (8) give the following values of the extinction level: 33.01 dB, 32.22 dB, 33.98 dB and 36.99 dB, respectively. For those magnitudes, the measurement error has been estimated as 0.82 dB, 0.81 dB, 0.85 dB and 0.95 dB, respectively [13].

The main advantage of this method is the possibility of performing measurements in an in-line system, *i.e.*, without leading out light from the optical fiber. This is especially important for measurements of fiber-optic polarizers because they usually operate in infrared range. An application of classic measurement systems involves difficult adjustment of the system. For this reason, approximation method is usually applied, *i.e.*, continuous measurement in the range from 1000 to 1275 nm and then the approximation of the curve obtained. The authors believe that proposed method is the only one allowing precise estimation of this parameter for 1300 and 1550 nm wavelengths.

4. Distributed security system based on the FOSI

The application of the FOSI to disturbance location has been presented in the paper of DAKIN [15]. This solution requires an additional Mach–Zehnder interferometer in an optical part of a device, however, it makes technical realisation difficult. In general, this sensor is based on experience gained from application of the phase

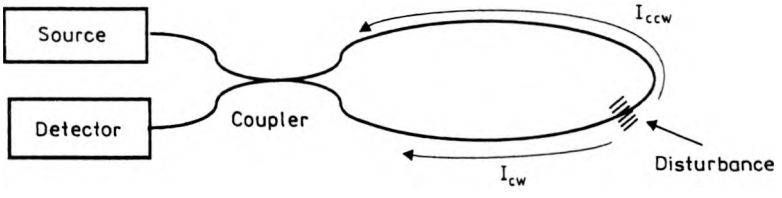

Fig. 13. FOSI as disturbed sensor.

modulator in the FOG system [16]. The disturbance, which appears at a point P of the FOSI with the fiber-optic loop length of L (Fig. 13), is modelled as a phase modulator with phase disturbance given by

$$\varphi(t) = \delta \sin(\omega t + \beta) \tag{9}$$

where δ stands for an amplitude of the phase disturbance, ω is a disturbance frequency, β is an initial phase of the disturbance. At the loop output one may obtain

two waves which propagate in opposite directions with amplitudes described by the expressions, respectively:

$$A_{cw} \approx A_0 \exp\{j\delta \sin[\omega(t+\tau_{max}-\tau)\}+\beta\}, \tag{10a}$$

$$A_{ccw} \approx A_0 \exp\{j\delta \sin[\omega(t+\tau)]+\beta\} \tag{10b}$$

where A_0 stands for the amplitude of incident beams in Sagnac interferometer loop, $\tau = (l_{ccw}n)/c$ – for a phase delay measured clockwise (cw) from a coupler for the access of the coupler by the counter-clockwise (ccw) beam, and $\tau_{max} = Ln/c$ is the time of light transition by the sensor loop.

The beams mentioned, in general, have different SOP due to a random birefringence of the optical fiber. The power of the signal interfering at the detector depends on the disturbance frequency ω, the length of loop L and the SOP of interfering beams [17]. Assuming adjusted condition of interference (parallel SOP of both beams), low frequency of disturbance, and loop length of a few thousand meters, detected power can be described as [18]

$$P_1(t) \approx P_0\{1+2\delta\omega(\tau_{max}/2-\tau)\cos[\omega(t+\tau_{max}/2)+\beta\}. \tag{11}$$

As one can see, the electric signal maintains the frequency ω of the disturbing signal and has the amplitude proportional to $2\delta\omega(\tau_{max}/2-\tau)$. Moreover, the detected signal decreases (up to zero in the middle of the loop) when τ increases.

The relationships derived have been experimentally verified in the system containing the classic FOSI. The system contained the loop 1000 m long rolled uniformly from coil to coil on a cylinder of 0.5 m in diameter. An acoustic loudspeaker has been used to induce oscillations. The loudspeaker has been moved along to the cylinder side at a constant distance from the cylinder surface. In Fig. 14**a**, theoretical results are presented. These have been obtained on the assumption of the Gaussian power distribution of enforcing wave. In Fig. 14**b**, the experimental results are presented. As one can see, experimental results confirm theoretical predictions.

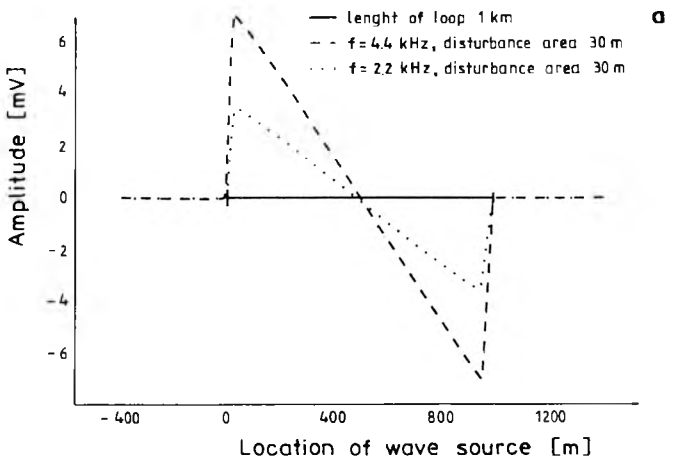

Fig. 14**a**

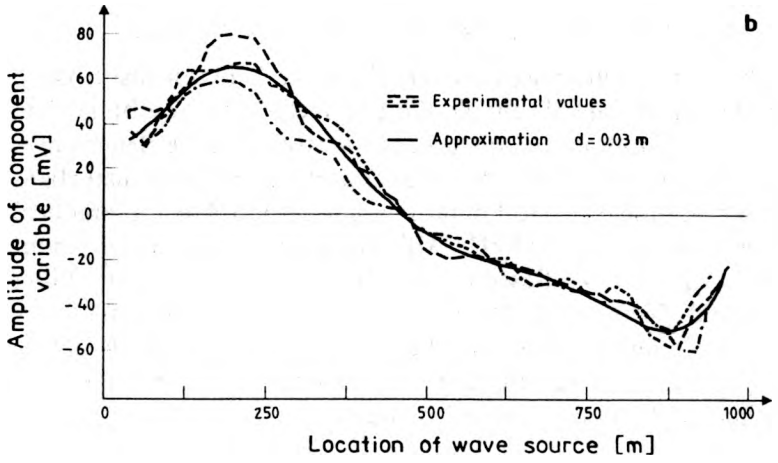

Fig. 14b

Fig. 14. Theoretical (**a**) and experimental (**b**) dependences of response signal on the disturbance location (P point), d — distanced between the source and the sensor loop.

The final Equation (11) is the basis for construction of disturbed sensor, which allows disturbance location. In Fig. 15, the idea of construction of such a sensor is presented [19]. The sensor consists of the double-loop Sagnac interferometer with the loops separated by a certain characteristic distance D, which depend on velocity of the propagation of disturbance wave in the medium surrounding the loop. For the soil at a temperature from 0 to 50 °C the distance D is about 2 cm. The essence of the loops' arrangement is their inverted placement, schematically marked in Fig. 15.

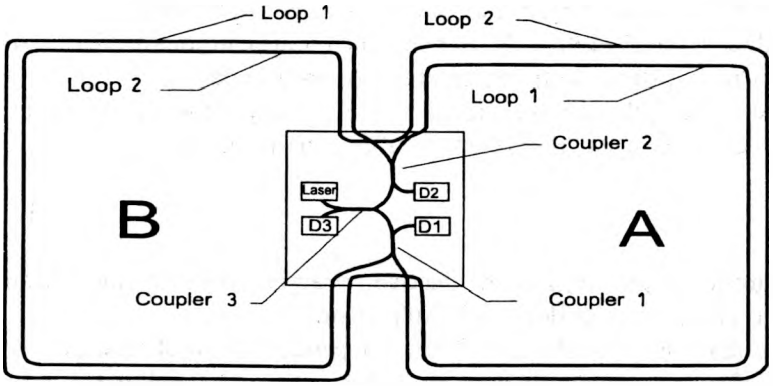

Fig. 15. Scheme of distributed sensor based on double-loop Sagnac interferometer [19].

For such an arrangement the following signals may be obtained on the detectors D1 and D2:

$$P_1(t) \approx P_0\{1+2\delta\omega(\tau_{max}/2-\tau)\cos[\omega(t+\tau_{max}/2)+\beta]\}, \tag{12a}$$

$$P_2(t) \approx P_0\{1+2\delta\omega\tau\cos[\omega(t+\tau_{max}/2)+\beta+\Delta\beta]\}, \quad \text{for } \tau < \tau_{max}/2, \tag{12b}$$

$$P_2(t) \approx P_0\{1+2\delta\omega(\tau-\tau_{max}/2)\cos[\omega(t+\tau_{max}/2)+\beta+\Delta\beta]\}, \quad \text{for } \tau > \tau_{max}/2 \quad (12c)$$

where $\Delta\beta$ stands for the phase shift caused by the difference between disturbance access time to both loops. Those signals enable the parameter τ to be obtained in a simple way and, by its recalibration, the disturbance location can be determined. The application of a suitable system of electronic signal processing allows disturbance location by the sensor. Optoelectronic limitations are responsible for practical possibilities of detection, namely, up to 20 kHz with an accuracy of location about 20 m for the loop length of 1 km [19]. Based on the above investigations, the Fiber Optic System for External Security of Objects (FOSESO) has been made by Szustakowski's group. This commercially available system can be used to obtain information concerning violation of security zone by an intruder, with the border length of the zone being up to two thousand meters.

5. FOSI as in-line measurement devices

A good environmental stability and possibility of applying short coherence source are the main advantages due to which the use of the FOSI as a measuring device is preferable. Below, the application of this interferometer for investigating fiber-optic phase modulator, nanometer vibration and measuring SOP of light are described.

5.1. Measurement of phase-amplitude characteristics

The FOSI may be easily adopted for the measurement of dynamic characteristic of fiber-optic phase modulator. The element is obtained by mounting a single-mode fiber on the piezoceramic moulder. Vibrations of the piezoceramic element cause a periodic change of the fiber geometry, hence, the relative phase modulation of the light wave propagated in the optical fiber. Moreover, such a measurement offers also opportunity to measure vibration with extremely low amplitude.

The application of sine enforcement signal to the phase modulator causes harmonic phase shift of light wave described by (9) with amplitude

$$\delta \approx \frac{2\pi}{\lambda} N_{eff} \Delta L \quad (13)$$

where λ is the wavelength of light, N_{eff} is an effective refractive index of the optical fiber, and ΔL is fiber elongation under field interaction.

In general, parameters β in (9) and δ in (13) may depend on several factors. For instance, in the case of piezoceramic element they depend on the voltage U, the enforcement frequency ω and on the construction of the element. Hence, measurement of the quantity (9) with known amplitude U and frequency ω, gives frequency-voltage characteristics of the phase modulator. Moreover, by application of (13) one can find ΔL and from this (based on the transducer construction) an amplitude of substrate vibration.

At the beginning of this paper, it has been said that the Jones' matrices for cw and ccw waves in the FOSI are in transposition relation. This is true for the optical

element independent of time in a linear medium, with the same modes at the input and output, while untrue for the existing Sagnac or Faraday effects. The above situation changes dramatically if the optical element is time-dependent. This is exactly the case of phase modulator harmonically dependent on time. In the case of ideal preparation, when the optic fiber is stiffly wound (without twist) on a piezo-ceramic moulder, the Jones matrix description of this element is as follows [6]:

$$\vec{\mathbf{M}} = \mathbf{D}[\eta\beta_0 a\{1+\alpha\sin(\omega t+\beta)\}]\,\mathbf{G}(\chi a\{1+\alpha\sin(\omega t+\beta)\}], \tag{14a}$$

$$\overleftarrow{\mathbf{M}} = \mathbf{D}[\eta\beta_0 a\{1+\alpha\sin[\omega(t-\tau)+\beta]\}]\mathbf{G}[\chi a\{1+\alpha\sin[\omega(t-\tau)+\beta]\}] \tag{14b}$$

where: **D** is the matrix of constant-phase retarder with phase shift $\eta a\beta_0$. The β_0 stands for propagation constant in fiber core, ηa – length of fiber joined to substratum, α – constant which is much more less than one, τ stands for retardation time of ccw beam signal in relation to cw beam signal.

Consequently, this time retardation between interacting beams causes change in system behaviour because, as may be shown even for linear input polarisation, the obtained result is [6]

$$m = 0.25\exp\{-j[(\delta-ba)[\sin(\omega t+\beta)+\sin[\omega(t-\tau)+\beta]]+2b]\} \tag{15}$$

where: $\delta = \eta\beta_0\alpha a$ stands for the amplitude of phase modulation (13), $b = \chi/a$ – for a constant related to the birefringence enforced in the fiber by its bending.

As one can see, phase modulator may in general introduce a constant phase shift $2b$ and two kinds of modulation. The first one is a phase modulation with amplitude of δ, the second one is the polarisation modulation with amplitude of $b\alpha$. For this reason, studies of dynamically changed phase element require that possibility of polarisation modulation be taken into consideration. In the system described, this requirement is fulfilled by an application of polarisation detector. Moreover, if the fiber is stiffly joined to the substrate, the above investigation can be used to study vibration with extremely low amplitudes.

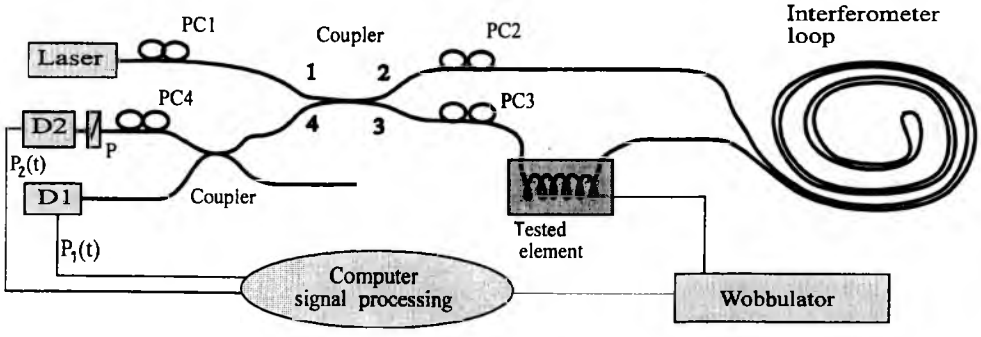

Fig. 16. Schematic view of the FOSI adapted for the study of elements [20].

A schematic view of the FOSI for such a measurement is shown in Fig. 16. Polarisation controller (PC1) placed in front of the coupler optimises conditions of

the induction of the sensor loop. The detection of output signal is performed in the 4th branch of the coupler. Introducing additional X-type coupler in this branch allows division of the output power to two detectors (D1 and D2). In the branch containing detector D2 preceded by the polarizer, an additional polarisation controller (PC4) is placed. This controller allows the output SOP and polarizer characteristic to be matched. In order to avoid the effect of Earth revolution and other disturbances on the measurement results, *i.e.*, Sagnac effect, the interferometer loop is coiled to the shape of double helix. The element under study is placed close to one of the ends of the interferometer loop. Two polarisation controllers (PC2 and PC3) placed inside the loop, allow adjustment of the working point of the system by an arbitrary modification of the polarisation properties of the loop [20].

For this configuration of the measuring system used to study phase element, one should adjust conditions of the system operation with the minimum polarisation modulation (at the level of detection system noise). This can be achieved by turning the controllers PC3 and PC2 and changing the element supplying voltage. In the case of this adjustment the signal on the detector D2 for an arbitrary adjustment the PC4 is assumed as $P_2(t) = 0$. In other words, polarisation modulation is neglected ($b\alpha \sim 0$) in (15), and additional all loop birefringence is compensated as well. Then the power detected by the detector D1 is [6]

$$P_1(t) = P_0\left\{1+\sin\left(\frac{\omega\tau}{2}\right)\cos\left[\omega\left(t-\frac{\tau}{2}\right)+\beta\right]\right\} \tag{16}$$

where P_0 stands for the power of semiconductor laser output signal.

Using this signal one can obtain the amplitude of phase disturbance generated by the phase element as

$$\Phi = \frac{(2n+1)\frac{\pi}{2}-(-1)^n\cos^{-1}[(P_1(t)/P_0)_{\max}]}{2\sin(\omega\tau/2)} \tag{17}$$

where n stands for successive signal maxima for which $P_1(t)/P_0 = 1$. Those extremes occur in case of amplitude Φ increase. It is easy to notice that the maximum of signal alternating component $P_1(t)$ on the basic enforcement frequency ω ($n = 0$) equals P_0 for amplitude increase Φ. Therefore, by measuring the maximum value $V_{\max pp}$ (just before sinusoid turn) one can normalise the signal $P_0 = V_{\max pp}$. From the above result with an additional assumption $n = 0$ we can obtain ΔL as

$$\Delta L = \frac{\lambda n\cos^{-1}[P_1(t)/V_{\max pp}]}{8\sin(\omega\tau/2)}. \tag{18}$$

In the measuring system (Fig. 17), the maximum voltage U applied to the element under study is adjusted by a wobbulator in such a way that the output remains linear. Then a chosen frequency range is swept by the wobbulator and the system output signal is registered by an A/D converter card on the IBM/PC. Due to the possibility of a mismatch occurring between the wobbulator and the element in

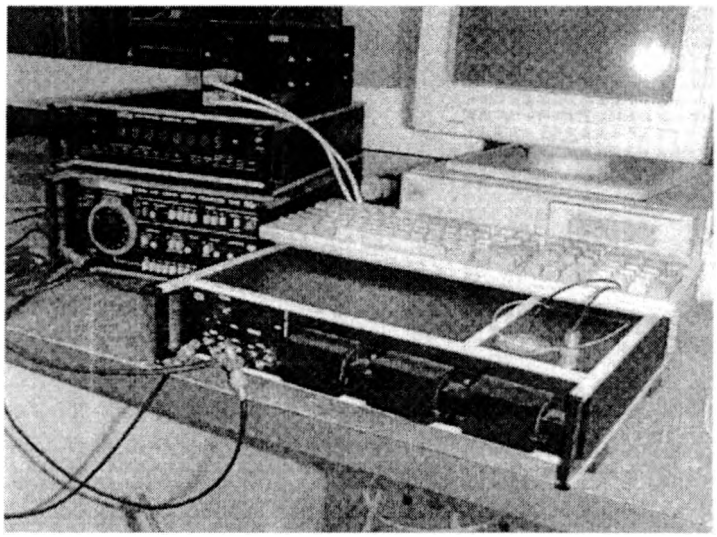

Fig. 17. General view of the FOSI used to measure phase of vibrating elements.

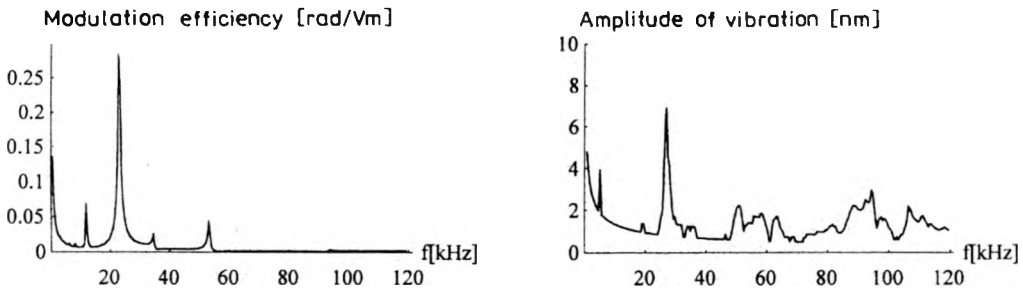

Fig. 18. Measured efficiency of phase modulator and the amplitude of vibration for element being tested [6].

question, additionally the load impedance of the system is registered. The phase shift $P_1(t)$ in relation to wobbulator signal describes unequivocally initial phase $\beta(V,\omega)$, because an argument of sine function in (16) differs from zero for the values of δ and ω different from zero.

Examples of phase modulator and vibration measurements are shown in Fig. 18. The phase modulator has been prepared by rigid mounting of a single-mode optic fiber 12.5 meters long on the hollow piezoceramic cylinder made from K-2 material. With the aid of the system, it is possible to obtain modulator parameters such as amplitude of phase disturbance δ [rad], initial phase β [rad], and modulation efficiency $\eta = \delta/(UL)$ [rad/Vm], all in frequency range $0.1-120$ kHz with 100 Hz resolution. A small loudspeaker has been used as a vibrating element being tested. It was a flat piezoceramic cylinder with a diameter of 20 mm and 1.25 mm thick. In order to measure those characteristics, the optic fiber has been mounted across the

diameter of the element under study on the length of 20 mm. By registering the output signal amplitude and load impedance vs enforcement frequency it is possible to obtain phase amplitude modulation vs enforcement frequency characteristics. Afterwards, using a simple equation of vibrating membranes, the amplitude on vibration in the centre of loudspeaker has been calculated.

5.2. Novel all-fiber ellipsometer

The polarisation phenomena existing in the FOSI system for measuring fiber-optic elements has been applied to a new concept of in-line optical fiber ellipsometer. The possibility of detecting changes of full SOP in fiber system is well known. There is a commercially available Hewlett–Packard device (giving information about changes of SOP by using Poincarè, Jones or Stokes representation) used mostly in laboratories for testing various fiber-optic elements [21]. However, this is a very expensive device and, due to a simple design, our measuring system is much compact and cheaper, hence more useful in practical application. The main idea of our solution is based on birefringence modulation in a standard single-mode fiber, and on identification of the input SOP changes by suitable detection of different harmonics of the output signal.

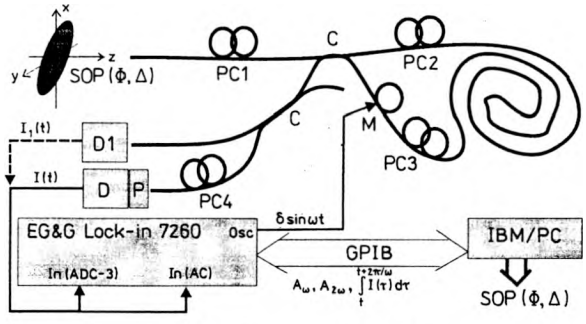

Fig. 19. Construction scheme of the FOSE.

The fiber-optic Sagnac ellipsometer (FOSE) is shown schematically in Fig. 19. This system is based on the FOSI shown in Fig. 16. The main differences are open input, fixed fiber-optic phase modulator (M) and new optoelectronic detection unit. The proper operation of the system requires orthonormal (opposite ellipticities and orthogonal azimuths) SOP of two interfering beams. This is achieved by nulling the first modulation harmonics of the signal $I_1(t)$ from the detector D1 by rotating the controllers PC1, PC2 and PC3. From the physical point of view, the birefringence of the interferometer loop is equivalent to the rotator by $\pi/4$ in this state. Then the final system adjustment is achieved by the maximal increase of the second harmonics of the signal $I(t)$ on the detector D by the controller PC4 [22].

Finally, the electrical signal generated by the detector D has the form

$$I(t) = 0.5B\left\{1-\sin(2\varphi)\left(\cos\Delta\cos\left(2\varphi\cos\left(\frac{\tau\omega}{2}\right)\sin\left(\omega t-\frac{\tau\omega}{2}\right)\right)\right)+\right.$$

$$+\sin\Delta\,\sin\left(2\delta\cos\left(\frac{\tau\omega}{2}\right)\sin\left(\omega t-\frac{\tau\omega}{2}\right)\right)\Bigg]\Bigg\}$$

$$=0.5B\Bigg\{1+\cos\Delta\sin 2\delta\Bigg[J_0\left(2\varphi\cos\frac{\tau\omega}{2}\right)+2\sum_{k=1}^{\infty}J_{2k}\left(2\delta\cos\frac{\tau\omega}{2}\right)\cos\left[2k\omega\left(t-\frac{\tau}{2}\right)\right]\Bigg]$$

$$+\sin\Delta\sin 2\delta\Bigg[2\sum_{k=0}^{\infty}J_{2k+1}\left(2\delta\cos\frac{\tau\omega}{2}\right)\sin\left[(2k+1)\omega\left(t-\frac{\tau}{2}\right)\right]\Bigg]\Bigg\} \tag{19}$$

where: B is the intensity-normalised factor and τ is retardation time of beams in the sensor loop.

The proper system performance requires the condition $J_0[2\delta\cos(\tau\omega/2)]=0$ to be fulfilled, hence an appropriate amplitude of the phase modulation δ generated by the modulator M. Then using the well-known technique for detection of the first and the second signal harmonics we are able to determine the searching parameters of SOP (see (4)) as:

$$\Delta=\tan^{-1}\left[\frac{A_\omega}{A_{2\omega}}\frac{J_2(2\delta\cos(\tau\omega/2))}{J_1(2\delta\cos(\tau\omega/2))}\right],$$

$$\Phi=\frac{1}{2}\sin^{-1}\left[\frac{1}{B}\sqrt{A_\omega^2+A_{2\omega}^2}\Big/\sqrt{\cos\Delta^2 J_2(2\delta\cos(\tau\omega/2))^2+\sin\Delta^2 J_1(2\delta\cos(\tau\omega/2))^2}\right] \tag{20}$$

where A_ω, $A_{2\omega}$ are amplitudes of the first and the second harmonics of the signal.

From the formulae presented above it is easy to determine changes in SOP by estimating the values of Φ and Δ in ranges of $0-\pi/4$ and $0-2\pi$, respectively. Moreover, as one can see from Fig. 20, the changes of Δ generally influence the ratio of signal harmonics, whereas changes of Φ affect the signal amplitude.

A 200 m long interferometric loop and low-voltage (~3 V) phase modulator at 22.3 kHz frequency have been used in the FOSE. The EG & G 7260 lock-in amplifier has been used as the main electronic equipment. As the output signal from this

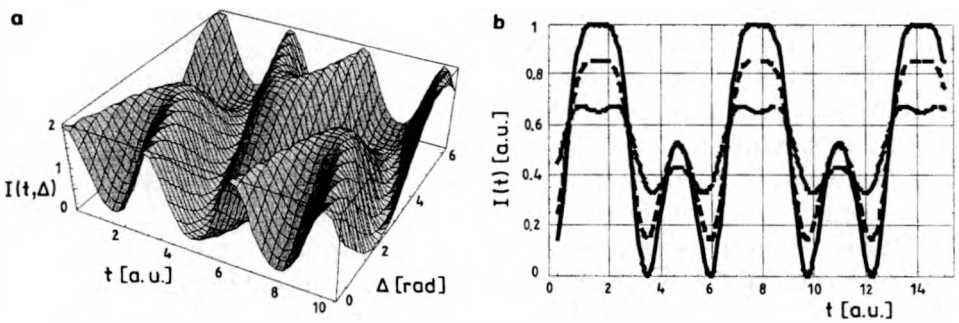

Fig. 20. Numerical simulation of ellipsometer signal for $\Phi=\pi/4$ (a), and chosen SOP (b), from top to bottom: ($\Delta=\pi/4$, $\Phi=3\pi/4$), ($\Delta=\pi/8$, $\Phi=3\pi/4$) and ($\Delta=\pi/18$, $\Phi=3\pi/5$), respectively.

device the amplitudes of the first and the second harmonics of the signal have been taken. Additionally, the lock-in amplifier gives also the intensity-normalised factor B, needed for calculation, as an integration signal $I(t)$ in the period $2\pi/\omega$. The same device is used to precisely drive the phase modulation, too.

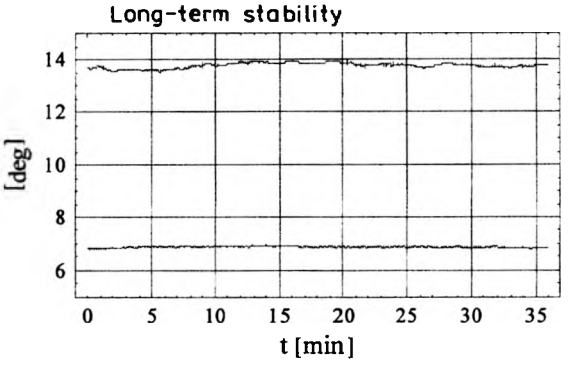

Fig. 21. Stability of the FOS operation. The input SOP measured by the BSC is $\Delta = 13.7$ deg (top curve) and $\Phi = 6.9$ deg (bottom curve).

Various input SOP, initially measured by the Babinet–Soleil compensator (BSC), have been used for testing purposes. The parameters Δ, Φ calculated on the basis of (20) in the system tested showed that the FOSE enables measurement of SOP with the accuracy of 0.09 deg and 0.03 deg for Δ and Φ, respectively. Such good results are due to generally high sensitivity of interferometric fiber-optic system. Moreover, in the after-math of reciprocal conditions its work the FOSE has good long-term stability as can be seen from Fig. 21. We thus expect this device to be useful for testing SOP changes in optical fiber applied in a coherent transmission system.

6. Summary and conclusions

The change of SOP in optical fiber is the main problem when constructing fiber-optic interferometers. The application of such devices as sensors requires that stabilisation of SOP of interacting beams be ensured. Usually, highly birefringent (HiBi) optical fiber is used for stabilising these states. However, this solution may be insufficient, because such a system is sensitive to a change of input beam SOP, and misalignment of birefringence axes in element connectors. Moreover, in normal sensor applications the interferometer arms can work in different environmental conditions, being thus the main source of system instability.

The FOSI is the most stable system, generally for two reasons. First, as regards the idea of construction, this system has arms of the same optical length. Second, the same fiber is used as a signal and a reference arm, which stabilises working conditions. Moreover, taking into consideration the possibility of birefringence changes, this configuration is sensitive only to rotation. Using HiBi fiber to its con-

struction and applying minimum configuration (common input-output and polarisation filter) one can obtain the system detecting only phase changes.

The investigations presented in this paper have been conducted over the last fifteen years at Physics Applications Department (PAD), Military University of Technology, Warsaw, Poland. All of them were connected with development of interferometric fiber-optic devices based on loop configuration. The main attention has been paid to understanding the polarisation behaviour of this configuration. Because of using the Jones calculus for the system description, the fully polarised light is assumed. However, there is a possibility of spreading out this description onto partially polarised light by applying the coherence matrix calculus, which uses the Jones description for fiber-optic elements. In the authors' opinion, the FOSI systems developed in PAD belong to four groups of devices, according to description provided in Sect. 3 – 5.

The technical parameters of DGS-13 appear advantageous as to be applied in a car navigation system. The improved laboratory FOG, type GS-13P, is successfully used to investigate slow-speed rotation platforms. Finally, the application of the FOSI as a security system has a commercial aspect. We believe that the idea of disturbance localisation may be realised in practice, too.

The presented FOSI application for measurement of phase modulator or fiber-optic polarizer characteristics gives highly reproducible results. The measuring system proposed exhibits high measurement stability. Moreover, it may be successfully applied to studies of measuring phase heads prepared in all-fiber technology. *e.g.*, for phase refractometer, with high reproducibility of results.

The system has been successfully adopted for studies of vibrations with very small amplitude (of nanometer order). The measurement of nanometer vibrations in a classical way is difficult and troublesome. This is caused by the necessity of using an interferometer system and depositing a reflective layer on the element under study in order to ensure proper operation of the interferometeric system. The application of the above described FOSI system does not require depositing reflective layers, but only the temporary mounting of the optic fiber segment.

The main idea of the FOSE based on the well-known technique allowed us to determine the Jones' vector by using a rotational quarter-wave plate and the polarizer. In the system, the rotational elements have been replaced by the fixed polarizer and the fiber retarder with a possibility to change its retardance. This approach considerably simplifies the measurement process, and enables quick determination of the parameters sought. The in-line system construction can be easily implemented in fiber links in the form of small and compact devices.

Acknowledgements – Some parts of this work, the main part of Sec. 2 and the whole of Subsec. 3.2 and 5.2 have been done under the financial support of the State Committee for Scientific Research (KBN), Grant No. 0T00A 017 14, and under the MUT Statutory Activity, No. ZNS-170.

References

[1] EZEKIEL S., ARDITTY H. J., *Fiber Optic Rotation Sensor and Related Technology*, Springer-Verlag, New York 1982.
[2] DAKIN J., CULSHAW B., *Fiber Optic Sensors*, Part IV, Artech House, Boston 1997.
[3] SZUSTAKOWSKI M., JAROSZEWICZ L. R., OSTRZYŻEK A., Optoelectron. Rev. **1** (1993), 38.
[4] JAROSZEWICZ L. R., P.L.Q. Thesis, Military University of Technology, Warsaw 1996.
[5] JAROSZEWICZ L. R., Proc. SPIE **3094** (1997), 204.
[6] JAROSZEWICZ L. R., KIEŻUN A., *Sensors and Their Applications VIII*, IOP Publ. Ltd., London 1997, p. 323.
[7] BERG R. A., Ph.D. Thesis, Standford University, London 1983.
[8] ADAMSKI W., JAROSZEWICZ L. R., SZUSTAKOWSKI M., Polish Patent, PL 167471 B1, 1995, Poland.
[9] JAROSZEWICZ L. R., Proc. SPIE **2729** (1996), 191.
[10] SZELMANOWSKI A., JAROSZEWICZ L. R., J. Tech. Phys. **39** (1998), 61.
[11] JAROSZEWICZ L. R., SZELMANOWSKI A., Proc. SPIE **3479** (1998), 284.
[12] SZELMANOWSKI A., JAROSZEWICZ L. R., Machine Dynamics Problems **22** (1998), 115.
[13] JAROSZEWICZ L. R., KIEŻUN A., Optoelectron. Rev. **3** (1995), 20.
[14] KINTER E. C., Opt. Lett. **6** (1981), 154.
[15] DAKIN J. P., PEARSE D. A. J., STRONG A. P., WADE C. A., Proc. SPIE **838** (1987), 325.
[16] BERG R. A., LEFEVRE H. C., SHAW H. J., Opt. Lett. **6** (1981), 502.
[17] SZUSTAKOWSKI M., JAROSZEWICZ L. R., Optoelectron. Rev. **2** (1994), 14.
[18] SZUSTAKOWSKI M., JAROSZEWICZ L. R., KIEŻUN A., Proc. SPIE **2341** (1994), 84.
[19] JAROSZEWICZ L. R., KIEŻUN A., SZUSTAKOWSKI M., ŚWIŁŁO M., Polish Patent, PL 173753, 1997, Poland.
[20] JAROSZEWICZ L. R., KIEŻUN A., SZUSTAKOWSKI M., Polish Patent, PL 174921 B1, 1998, Poland.
[21] CROSS R., HEFFNER B., HERNADAY P., Laser Optoelectron. **11** (1991), 37.
[22] JAROSZEWICZ L. R., KIEŻUN A., ŚWIŁŁO R., sent to OFS-13 Conf. Korea, 1999.

Received November 16, 1998
in revised form January 28, 1999